Two-Parametrical Control of Series Resonant DC-DC Converters that Operate with Common Load

Aleksandar Vuchev[1] and Nikolay Bankov[2]

Abstract – **A control technique is investigated for two series resonant DC-DC converters that operate with common load. In order to reduce the inverter currents a change of both operating frequency and phase shifting together is used. On the base of existing analyses output and control characteristics are built. The obtained results are confirmed by computer simulations.**

Keywords – **Series Resonant DC-DC Converters, Frequency Control, Phase Shift Control.**

I. INTRODUCTION

Series resonant DC-DC converters working above resonant frequency have been widely used recently. A well-known method for the output power control is the phase shift control technique [1÷4]. Constant operating frequency is the main advantage of it. This control technique is based on the simultaneous operation of two inverters the output voltages or currents of which are phase-shifted. Therefore, two converter topologies are available: a series and a parallel one.

When the series topology is in use, the two inverters are connected in series to a common load [3, 4]. As a result, the converter output voltage equals the sum of the output voltages of the inverters. The inverter currents are equal and depend on the load. A main disadvantage of this topology is the inability of no-load mode. It is well-known that the output current decrease causes the resonant inverter to stop working.

The parallel topology requires both the inverters to be connected in parallel to the load [2]. In this case the load current equals the sum of the inverter output currents. The main advantage is that the load resistance increase does not cause compulsory work stop. It is well-known that as the phase-shift angle increases, the inverters begin sharing energy to each other, remaining their output current values high enough. Therefore, at certain conditions the converter work is preserved even in no-load mode. At very big phase-shift angles, however, the output currents of the inverters have significant values. Violating the condition the operating frequency to be constant is one of the ways of elimination of this drawback.

Purpose of this paper is a DC-DC converter based on series resonant inverters connected in parallel to a common load to be examined at change of both phase-shifting and operating frequency change together. The investigation is based on the results of existing analyses of series resonant converters operating above the resonant frequency at phase-shift control.

[1]Aleksandar Vuchev is with the Department of Electrical Engineering and Electronics, Technical Faculty, University of Food Technologies, 26 Maritza Blvd., 4002 Plovdiv, Bulgaria, E-mail: avuchev@yahoo.com

[2]Nikolay Bankov is with the Department of Electrical Engineering and Electronics, Technical Faculty, University of Food Technologies, 26 Maritza Blvd., 4002 Plovdiv, Bulgaria, E-mail: nikolay_bankov@yahoo.com

II. CONVERTER EQUIVALENT CIRCUITS

The circuit of the examined converter is presented in fig.1. Two half-bridge resonant inverters and an uncontrollable rectifier are its main modules.

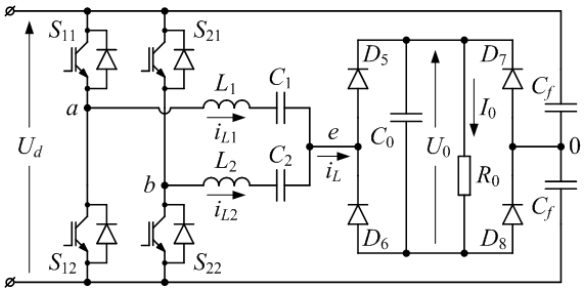

Fig.1. Circuit of the resonant DC-DC converter

With the conventional phase-shift control of the output power the switches of the first inverter (S_{11}, S_{12}) conduct in opposite at an operating frequency f_S. The switches of the second inverter (S_{21}, S_{22}) work in the same way. The control impulses applied to S_{11} and S_{21} (respectively S_{12} and S_{22}) are phase-shifted to an angle α. The two half-bridge inverters have one common node (node **0**). Hereby, two square-wave voltages, shifted one towards another at angle α, are generated between point **0** and points ***a*** and ***b*** respectively. Their amplitude equals half of the supply voltage ($U_d/2$).

As the two resonant inverters work at the same frequency f_S, it is necessary that $L_1 = L_2 = L$ и $C_1 = C_2 = C$. Thus, the resonant frequency, the characteristic impedance and the frequency detuning for the two resonant circuits are:

$$\omega_0 = 1/\sqrt{LC}\,; \quad Z_0 = \sqrt{L/C}\,; \quad \nu = 2\pi f_S/\omega_0 = \omega_S/\omega_0 \quad (1)$$

In [5] it is shown, that the operation of the converter can be examined on the basis of the equivalent circuit shown in fig.2a. Because of the parallel connection between the two inverters the resonant frequency does not change but the characteristic impedance is reduced twice:

$$Z_{0PAR} = \sqrt{L_{EQ}/C_{EQ}} = 0{,}5\sqrt{L/C} = 0{,}5Z_0 \quad (2)$$

The circuit in fig.2a corresponds to a converter, realized with the series topology. The voltage u_{SW} is as a result of the operation of the inverter switches. It has a quasi-square wave-

form and amplitude equal to $U_d/2$. On the other hand, the voltage u_0 corresponds to the commutations in the rectifier. It has a square wave-form, switching between $\pm U_0$, and is phase-locked with the inductor current i_L.

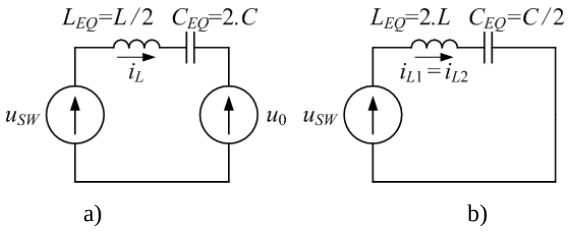

Fig.2. Equivalent Circuits

In no-load mode, current to the input of the rectifier does not flow. In this case, the energy is exchanged only between the inverters and the examination can be conducted on the base of the equivalent circuit shown in fig.2b. The characteristic impedance for this circuit increases twice:

$$Z_{0SER} = \sqrt{L_{EQ}/C_{EQ}} = 2\sqrt{L/C} = 2Z_0 \qquad (3)$$

This circuit corresponds to a converter realized with a series topology in short circuit mode. In this case, the voltage u_{SW} has amplitude that equals the supply voltage U_d.

III. Converter Operating Modes

In order to simplify the analysis and the obtaining of generalized results, all the parameters related to the examined converter are normalized:

- voltages towards $U_d/2$;
- currents towards $U_d/2Z_0$;
- resistances towards Z_0.

As the equivalent circuits (fig.2) correspond to a converter realized with a series topology, results from existing analyses of series resonant DC-DC converters with phase-shift control can be applied. Thus, in [3] two main operating modes of the converter are defined. They are determined according to the commutation mechanisms of the inverter switches – with zero-voltage switching or with zero-current and zero-voltage switching. The analysis presented in [4] shows, however, that the second of these modes is divided to two sub-modes, which is related to the appearance of current pauses (discontinued current mode) in the operation of the rectifier. For the so determined modes, the operation of the converter is illustrated in fig.3. It presents normalized wave-forms of the inverter voltage u_{SW}, the rectifier input voltage u_0, the voltage u_C across the capacitor C_{EQ} and the current i_L through the inductor L_{EQ}.

In ***MODE I***, both the inverters deliver energy to the rectifier. This case can be observed at small values of the load resistor R_0.

In ***MODE II*** and ***MODE III***, as one of the inverters delivers energy to the rectifier, the other returns part of this energy back to the supply. This case can be obtained with increase of the value of R_0. At significant values of the load resistor (***MODE III***), discontinued current mode is available.

Regardless of the operating mode, three commutations can be observed during a half-period – two for the voltage u_{SW} and one for the voltage u_0. In this way, three working intervals are formed, at the time of which a voltage u_{EQ} is applied to the resonant circuit.

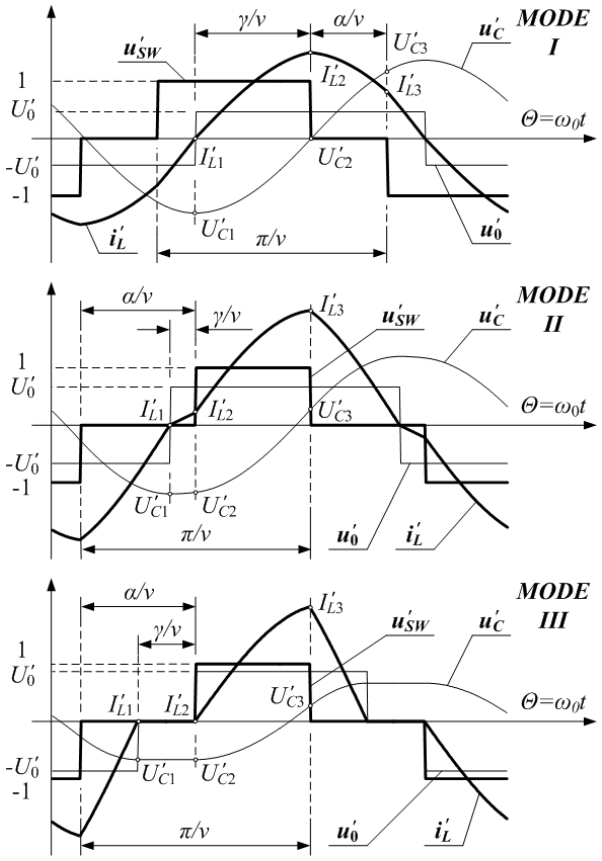

Fig.3. Waveforms for different operating modes

For the operating frequency ω_S in fig.3, the angle of the first interval is labeled with γ. At the beginning of this interval, the inductor current i'_L equals zero (I'_{L1}=0), and the capacitor voltage u'_C – negative peak value (U'_{C1}=-U'_{CM}). The normalized values of the voltages U'_{EQ} and the interval angles Θ_W for the resonant frequency ω_0 are presented for the different modes in Table I.

TABLE I
OPERATING INTERVAL'S PARAMETER DESCRIPTION

Case	Parameter	Interval		
		1	2	3
MODE I	Θ_W	γ/ν	α/ν	$(\pi-\alpha-\gamma)/\nu$
	U'_{EQ}	$1-U'_0$	$-U'_0$	$-1-U'_0$
MODE II	Θ_W	γ/ν	$(\pi-\alpha)/\nu$	$(\alpha-\gamma)/\nu$
	U'_{EQ}	$-U'_0$	$1-U'_0$	$-U'_0$
MODE III	Θ_W	γ/ν	$(\pi-\alpha)/\nu$	$(\alpha-\gamma)/\nu$
	U'_{EQ}	$-U'_{CM}$	$1-U'_0$	$-U'_0$

From the presented in [5] analysis and in accordance with the equivalent circuit in fig.2a, for the *j*-numbered interval the

inductor current i'_L and the capacitor voltage u'_C are expressed as follows:

$$i'_L(\Theta) = I'_{L\,j}\cos\Theta - \left(U'_{C\,j} - U'_{EQ\,j}\right)\sin\Theta / 0{,}5 \qquad (4)$$

$$u'_C(\Theta) = 0{,}5I'_{L\,j}\sin\Theta + \left(U'_{C\,j} - U'_{EQ\,j}\right)\cos\Theta + U'_{EQ\,j} \qquad (5)$$

In the above expressions j is the interval number; I'_{Lj} and U'_{Cj} are the initial values of the current i'_L and the voltage u'_C; U'_{EQj} - the equivalent voltage acting upon the resonant circuit during the interval; $\Theta=0\div\Theta_{Wj}$; Θ_{Wj} – angle corresponding to the interval duration.

In fig.3 it can be seen that the value of i'_L at the end of the examined interval appears to be the initial value of the next one. The same thing is valid for the voltage u'_C. Then:

$$I'_{L\,j+1} = I'_{L\,j}\cos\Theta_{W\,j} - \left(U'_{C\,j} - U'_{EQ\,j}\right)\sin\Theta_{W\,j} / 0{,}5 \qquad (6)$$

$$U'_{C\,j+1} = 0{,}5I'_{L\,j}\sin\Theta_{W\,j} + \left(U'_{C\,j} - U'_{EQ_j}\right)\cos\Theta_{W\,j} + U'_{EQ\,j} \qquad (7)$$

Baring in mind that at the end of the third interval the inductor current equals zero again, and the capacitor voltage reaches positive peak value, on the base of (6) and (7) the following expressions are obtained:

$$-U'_{CM} = \frac{\sum_{j=1}^{3} U'_{EQ\,j}\left[\sin\left(\frac{\pi}{\nu} - \sum_{i=1}^{j}\Theta_{W\,i}\right) - \sin\left(\sum_{i=j}^{3}\Theta_{W\,i}\right)\right]}{\sin\frac{\pi}{\nu}} \qquad (8)$$

$$U'_{CM} = \frac{\sum_{j=1}^{3} U'_{EQ\,j}\left[\cos\left(\sum_{i=j}^{3}\Theta_{W\,i}\right) - \cos\left(\frac{\pi}{\nu} - \sum_{i=1}^{j}\Theta_{W\,i}\right)\right]}{1+\cos\frac{\pi}{\nu}} \qquad (9)$$

Equations for normalized values of both the capacitor peak voltage U'_{CM} and the output voltage U'_0 are obtained from these expressions. Thereafter, the initial values I'_{Lj} and U'_{Cj} can be calculated by means of (6) and (7). On the base of expression (4), an equation for the average output current I'_0 is obtained:

$$I'_0 = \frac{\nu}{0{,}5\pi}\sum_{j=1}^{3}\frac{I'_{L\,j}\sin\Theta_{W\,j}}{2} -$$

$$-\frac{\nu}{0{,}5\pi}\sum_{j=1}^{3}\left(U'_{C\,j} - U'_{EQ\,j}\right)\left(1-\cos\Theta_{W\,j}\right) \qquad (10)$$

By proper integration, expressions for the average and root means square (RMS) values of the currents through the different circuit elements can also be obtain on the base of equation (4).

IV. Control Technique

In accordance with the equivalent circuit in fig.2b and on the base of the results from the analyses, presented in [4, 5], expressions for the RMS values of the inverter inductor currents are obtained.

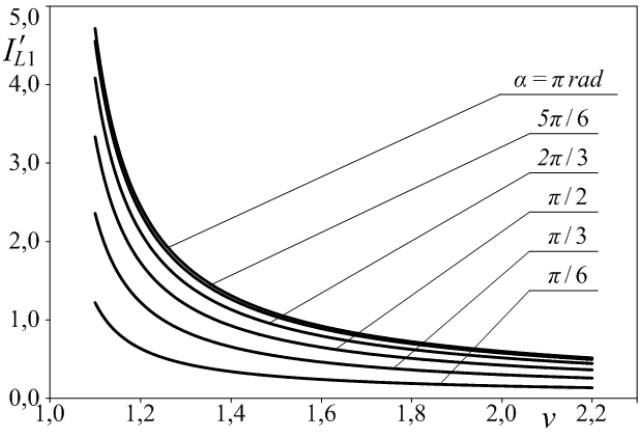

Fig.4. Normalized RMS value of the inductor current I'_{L1} as function of frequency detuning ν

Fig.4 presents the normalized dependencies of the inductor current RMS value of the first inverter on the frequency detuning ν, when the converter operates in no-load mode. These dependencies are obtained for different values of the phase-shift angle α. The characteristics for the second inverter are analogous. Fig.4 shows that when the converter works in no-load mode at low frequency, the stresses over the circuit elements may be significant. A solution to this problem is increase of the operating frequency. It can be observed that increasing the operating frequency only twice results in significant decrease of the coil currents. However, this causes reduction of the converter efficiency.

In order to maintain the efficiency of the converter at high output power and to reduce the stresses over the elements at small loading, a normalized control variable CP is introduced to change simultaneously two parameters – the phase-shift angle α and the working frequency f_S:

$$\alpha = (1-CP)\pi\,, \quad f_S = f_L + (1-CP)(f_H - f_L) \qquad (11)$$

When CP is changed from 0 to 1, α changes from π to 0 and f_S changes from a minimum value f_L to a maximum value f_H.

On the base of equations (1) and (12), a minimum νL and a maximum value νH for the frequency detune can be defined.

V. Output and Control Characteristics

As a result of the presented analysis and in accordance with the proposed control strategy, the output and control characteristics are drawn for the examined converter. It is assumed for the range of the frequency detuning that ν_L=1,1 и ν_H=2,2. From the analysis presented in [5], it can be proved that at ν_H>2 only two of the mentioned operating modes are possible – ***MODE I*** and ***MODE II***.

Fig.5 presents the normalized output characteristics (with thick curves) obtained for several values of the control parameter CP=[0,2; 0,4; 0,6; 0,8; 0,9; 0,95]. The boundary between the operating modes is drawn with dotted curve. The

characteristics are similar to those at conventional phase-shift control.

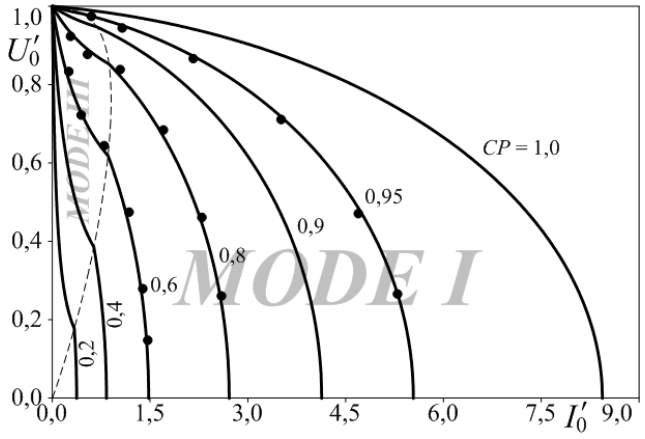

Fig.5. Load characteristics of the converter

Fig.6 presents the normalized control characteristics (with thick curves). They are obtained for several values of the load resistor ($R'_0=U'_0/I'_0$). The boundary between the working modes is drawn with dotted curve. At high values of the load resistor ($R'_0\geq1$) the characteristics are similar to those at conventional phase control. At low values ($R'_0<1$), however, their shape is different.

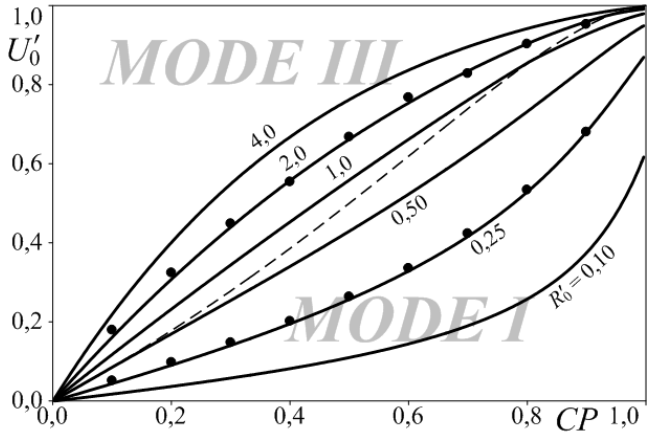

Fig.6. Control characteristics of the converter

The analysis of the two figures shows several main differences compared to the conventional phase-shift control [3, 4]:

1. The range of ***MODE I*** is increased (fig.5), which is a premise for improvement of the converter efficiency;

2. At low values of the control parameter *CP*, the more significant influence is that of the operating frequency, while at high values it is the phase-shift angle α that influences more.

3. At low values of the load resistor ($R'_0<1$), increase of the control parameter *CP* results an increased gradient of the control characteristics.

In order to verify the theoretically obtained results, simulations with OrCAD PSpice are done. A converter based on parallel topology is modeled for this purpose. The main specifications of this prototype are: U_d=300V; f_L=50kHz; f_H=100kHz; $L_1=L_2$=204,223μH; $C_1=C_2$=60nF; Z_0=58,357Ω; CP=0÷1 ($\alpha=\pi\div0$; ν=1,1÷2,2).

On the base of operation in steady state mode, normalized values of the output voltage U'_0 and current I'_0 are obtained. The results obtained at CP=[0,6; 0,8; 0,95] and R'_0=[0,1; 0,2; 0,4; 0,8; 1,6; 3,2] are entered as dots in the area of the output characteristics. Analogically, normalized values of the voltage U'_0 are obtained at R'_0=[0,25; 2,00] and CP=[0,1; 0,2; 0,3; 0,4; 0,5; 0,6; 0,7; 0,8; 0,9]. They are entered as dots in the area of the control characteristics.

The comparison done in this way shows very good match between the results from the theoretical analysis and those from the simulation examinations.

VI. Conclusion

A DC-DC converter consisting of two series resonant inverters connected in parallel to a common load (a rectifier) is examined. In order to maintain its efficiency at high output power, as well as, to reduce the stresses over the elements at lower loading, the control is realized by the simultaneous change of two parameters – the phase-shift between the currents of the two inverters and their operating frequency.

On the base of results from existing analyses, the converter work above the resonant frequency is examined. As a result, output and control characteristics are drawn. The comparison between these characteristics and those at conventional phase-shift control shows several essential differences. The authenticity of the theoretical examination is confirmed by computer simulations.

The obtained results can be used for design of DC-DC converters similar to the examined one.

References

[1] Y. Cheron, H. Foch, J. Roux, *Power Transfer Control Methods in High Frequency Resonant Converters*, PCI Proceedings, Munich, 1986, pp 92-103.

[2] P. Savary, M. Nakaoka, T. Maruhashi, "Novel Type of High-Frequency Link Inverter for Photovoltaic Residental Applications", Vol. 133, Pt. B, No. 4, pp. 279-284, July 1986.

[3] Sabate J.A., F.C. Lee, *Zero-Voltage Switching with Fixed Frequency Clamped-Mode Resonant Converters*, Proceedings of Virginia Power Center Seminar, 25-27 September 1989, pp.83-91.

[4] B. S. Nathan, V. Ramanarayanan. "Analysis, Simulation and Design of Series Resonant Converter for High Voltage Applications", Industrial Technology 2000. Proceedings of IEEE International Conference, Vol. 1, pp. 688-693, 19-22 Jan. 2000.

[5] A. Vuchev, N. Bankov, "Analytical Modeling and Investigation of Phase Shift Controlled Resonant DC-DC Converter", Engineering Sciences, Journal of the Bulgarian Academy of Sciences, 2010, № 2, pp. 36-50.